

Investigation of Solid State Synthesis and Characterizations of Novel Sodium Rare-Earth Oxyphosphates

Semih SEYYİDOĞLU¹, Macit ÖZENBAŞ², Aysen YILMAZ^{1*}

¹*Department of Chemistry, Middle East Technical University, 06531, Ankara-TURKEY*

²*Department of Metallurgical and Materials Engineering, Middle East Technical University, 06531, Ankara-TURKEY*
e-mail: ayseny@metu.edu.tr

Received 06.12.2006

A new orthorhombic phase of Na₂LaOPO₄ (sodium lanthanum oxyphosphate), and novel Na₂NdOPO₄ (sodium neodymium oxyphosphate), Na₂SmOPO₄ (sodium samarium oxyphosphate) were synthesized by solid state reactions of Na₂CO₃, NH₄H₂PO₄, and Ln₂O₃

(Ln = La, Nd, and Sm). The unit cell dimensions were calculated using their X-ray powder diffraction data, which were a = 13.60(1), b = 12.71(1), and c = 6.96(1) Å, a = 13.466(5), b = 12.547(6), and c = 6.932(5) Å, and a = 13.54(1), b = 12.577(8), and c = 7.047(5) Å, respectively, and the probable space group was Pmm2. Using the same procedure orthorhombic Na₂DyOPO₄ (sodium dysprosium oxyphosphate), Na₂HoOPO₄ (sodium holmium oxyphosphate), Na₂ErOPO₄ (sodium erbium oxyphosphate), and Na₂YbOPO₄ (sodium ytterbium oxyphosphate) were also prepared for the first time in this work. The IR data of the compounds agreed with the values given in the literature. The Raman data and SEM micrographs of the synthesized compounds are given for the first time in this report.

Key Words: Oxyphosphates, Rare-earths, Sodium Rare Earth Oxyphosphate, Raman, powder XRD, SEM.

Introduction

For several reasons related to potential applications, such as ionic conductivity or superconductivity, non-linear optical properties, ferro-electricity, magnetism, laser properties, catalytic activity, etc., the following compounds are still currently being investigated: KTiOPO₄ (KTP),¹ NbOPO₄,² BiCoPO₅,³ VOPO₄.3H₂O,⁴ Pb₂BiO₂PO₄,⁵ and Bi_{~6.2}Cu_{~6.2}O₈(PO₄)₅.⁶

*Corresponding author

Among these oxyphosphates, potassium titanyl oxyphosphate (KTiOPO₄) (KTP) crystals exhibit excellent nonlinear optical properties in the visible range because of their high nonlinear coefficients and wide acceptance of temperature and angular fluctuations. High thermal stability, good mechanical characteristics, transparency over a large wavelength range, large nonlinear optical coefficients, high damage threshold, and broad angular acceptance of KTP have made it the standard material for several industrial and medical applications.

KTP has an orthorhombic structure and belongs to the acentric point group mm2 (space group Pna2₁), and each cell contains 8 formula units. Its structure consists of PO₄ tetrahedra and TiO₆ octahedra with potassium in larger voids. TiO₆ octahedra are strongly distorted and the Ti-O bonds are short, which are believed to be the prime cause of the nonlinear properties of KTiOPO₄. This family of compounds is generalized as MM^IOXO₄, where M may be K,⁷ Rb, or Ni,⁸ and M^I may be Ti, Nb,^{9–11} Nd,¹² Sn, Mg,¹³ or a combination of 2 of these ions; X may be P or As.¹⁴

Doping these crystals with rare earth ions is interesting because the matrix can be merged to achieve self-induced effects. In the paper published by Diaz, the effect of Er- and Yb-doping on Nb:KTP crystals were investigated.^{15,16}

As these materials seem to offer promising directions for future research, KTP^{17,18} and its many isostructural compounds constitute a large field of research. In the work done by Zhang, an effective blue coherent laser was obtained using Ce:KTP crystals.¹⁹ Diaz and coworkers studied the photoluminescent properties of Er- and Nd-implanted KTP, and RTP crystals,^{20,21} and the optical absorption of Nd³⁺ in KTP single crystals; those co-doped with Al, Na, and W have also been studied.^{22,23} In addition to these, many researchers have worked on the mechanical,²⁴ and optical^{25–28} properties of KTP, RTP, and Nb:KTP.

As rare earth phosphates (*Re*PO₄) have a wide range of potential applications for optical materials, including laser, phosphors, and more recently, anti UV-materials, in the form of powders, coatings, or dense sintered parts, they have become the focus of growing interest during the past few years and numerous researchers have recently become devoted to these compounds.^{29–32} Champion's group reported the synthesis, characterization³³ and thermal³⁴ behavior of *Re*PO₄.H₂O, while Nariai synthesized *Re*PO₄.H₂O using rare earth elements, where Re = La, Ce, and Nd, and oxide, carbonate, chloride, nitrate, sulphate, oxalate, and fluoride are anions.³⁵

While numerous reports exist in the literature dealing with the synthesis, characterization, and properties of KTP and related materials, there are only few reports regarding the preparation of rare earth oxyphosphates, some of which possess a KTP-type structure. A report by Kizilyalli showed the presence of 2 orthorhombic rare earth oxyphosphates, i.e. Na₂GdOPO₄³⁶ and Na₂LaOPO₄,³⁷ however, no attempt to synthesize other sodium rare earth oxyphosphates has been reported in the literature. Herein we present research conducted on the solid state reactions between sodium carbonate, rare earth (III) oxide, and ammonium dihydrogen phosphate, as formularized below:



Unfortunately, our all experiments to obtain single crystal products failed and it is not possible to find structural data about the related compounds in the literature to perform Rietveld analysis for a structural solution. This manuscript is the first to report the synthesis and powder diffraction data of new sodium rare earth oxyphosphates.

Experimental Details

Chemical Substances

The following solid powders were used in the solid state reactions of various rare earth oxides: La_2O_3 , Nd_2O_3 , Sm_2O_3 , Gd_2O_3 , Dy_2O_3 , Ho_2O_3 , Er_2O_3 , Yb_2O_3 , Na_2CO_3 , and $\text{NH}_4\text{H}_2\text{PO}_4$ (from Merck, Fluka, Aldrich, and Sigma).

Instrumentation

XRD structural analyses of the products were performed on an Rigaku Miniflex X-ray diffractometer equipped with $\text{Cu K}\alpha$ (30 kV, 15 mA, $\lambda = 1.54051 \text{ \AA}$) radiation at room temperature. Scanning was performed between 5° and 90° 2θ , generally. All measurements were made with 0.05° steps at the rate of $0.5^\circ \text{ min}^{-1}$. The divergence slit was variable, and scattering and receiving slits were 4.2° and 0.3 mm , respectively. The precise peak positions in the X-ray powder patterns of the samples were determined by means of the fitting program, CELREF,³⁸ yielding the least squares refinement of the lattice parameters.

The vibrational modes of the molecules in the samples were defined with the help of a Nicolet 510 FTIR infrared spectrometer in the region of $400\text{-}2000 \text{ cm}^{-1}$. Spectroscopic grade KBr was used for making IR pellets. KBr was dried at 180°C for about 1 d before use. Jobin Yvon-Horiba was used for Raman scattering spectra. This instrument has an He-Ne laser wavelength of 632.83 nm and a Peltier cooled CCD detector. Laser power was 10 MW and the detector was operated at -75°C . The slit width was $200 \mu\text{m}$ and grating with $600 \text{ blazes cm}^{-1}$ was used. Data accumulation duration was 60 s, and each accumulation was performed 5 times. Scanning electron micrographs were taken at 20 kV with a JEOL JSM 6400 equipped with an energy dispersive spectrometer (EDS). The solid state reactions were carried out in air with the aid of muffle furnaces.

Experimental Procedure

All preparations were made by spontaneous crystallization with stoichiometric proportions of the reactants in an oxygen atmosphere with the following formula:



The composition of each mixture and heat treatment are given in Table 1. Desired quantities of salts and oxides were weighed separately and crushed well in an agate mortar. Then, the mixtures were transferred into a porcelain crucible and put into a furnace for heating at 500°C for 11 h, 700°C for 10 h, 800°C for 5 h, 850°C for 5 h, 900°C for 15 h, 950°C for 25 h, and 1100°C for 15 h. The heating rate of the furnaces was $750^\circ \text{C h}^{-1}$. The products were taken from the furnaces directly to outside. The starting material weight was 1.0004 g for La_2O_3 , Nd_2O_3 , Sm_2O_3 , Gd_2O_3 , Dy_2O_3 , Ho_2O_3 , Er_2O_3 , and Yb_2O_3 . Weight losses of the products are in good agreement with the theoretical ones. The products were subjected to X-ray diffraction and IR analysis after each sintering process.

Results and Discussion

After a final heating period at 1100 °C, X-ray diffraction patterns of the products were obtained and the final orthorhombic compounds were divided into 2 sets. In the X-ray diffraction pattern of the first set (Figure 1), Na₂LaOPO₄, Na₂NdOPO₄, and Na₂SmOPO₄ products were separated according to their splitting peak, as presented by Kizilyalli.³⁷ The second set, Na₂GdOPO₄, Na₂DyOPO₄, Na₂HoOPO₄, Na₂ErOPO₄, and Na₂YbOPO₄ were also indexed in an orthorhombic system without having a splitting peak in their XRD pattern (Figure 2).

Table 1. Heating conditions and composition of the mixtures.

Na ₂ LnOPO ₄	Na:Ln:P	500 °C	700 °C	800 °C	850 °C	900 °C	950 °C	1100 °C
Na ₂ LaOPO ₄	2:1:1	11 h	10 h	5 h	5 h	15 h	25 h	15 h
Na ₂ NdOPO ₄	2:1:1	11 h	10 h	5 h	5 h	15 h	25 h	15 h
Na ₂ SmOPO ₄	2:1:1	11 h	10 h	5 h	5 h	15 h	25 h	15 h
Na ₂ GdOPO ₄	2:1:1	11 h	10 h	5 h	5 h	15 h	25 h	15 h
Na ₂ DyOPO ₄	2:1:1	11 h	10 h	5 h	5 h	15 h	25 h	15 h
Na ₂ HoOPO ₄	2:1:1	11 h	10 h	5 h	5 h	15 h	25 h	15 h
Na ₂ ErOPO ₄	2:1:1	11 h	10 h	5 h	5 h	15 h	25 h	15 h
Na ₂ YbOPO ₄	2:1:1	11 h	10 h	5 h	5 h	15 h	25 h	15 h

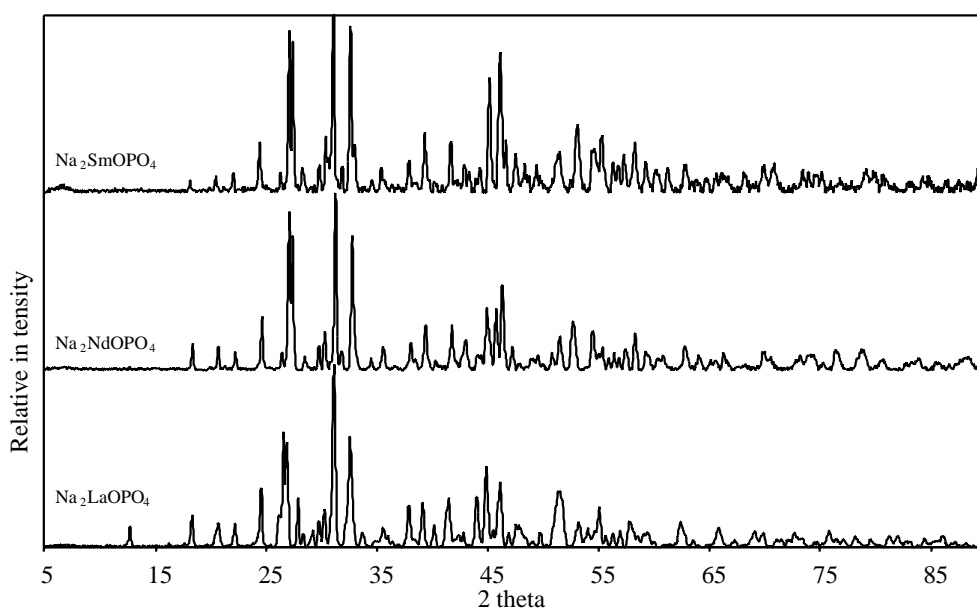


Figure 1. X-ray powder diffraction patterns of set 1.

XRD Studies

In the synthesis of both sets, the XRD patterns of the products showed great similarity, but they were not the expected products for all the experiments performed at 900 °C for a 15-h time interval. As the reaction proceeded at 950 °C for 25 h, solid state reactions at these stages also did not give the expected products.

The IR spectra of the products obtained at these temperatures supported this idea. Therefore, to obtain the desired products the temperature was increased. Prolonged heating of the products at 1100 °C (three 5-h periods and grinding in between) resulted in 1 phase product, which was orthorhombic – Na₂LnOPO₄ (where Ln = La, Nd, and Sm). The XRD patterns of set 1 are presented in Figure 1.

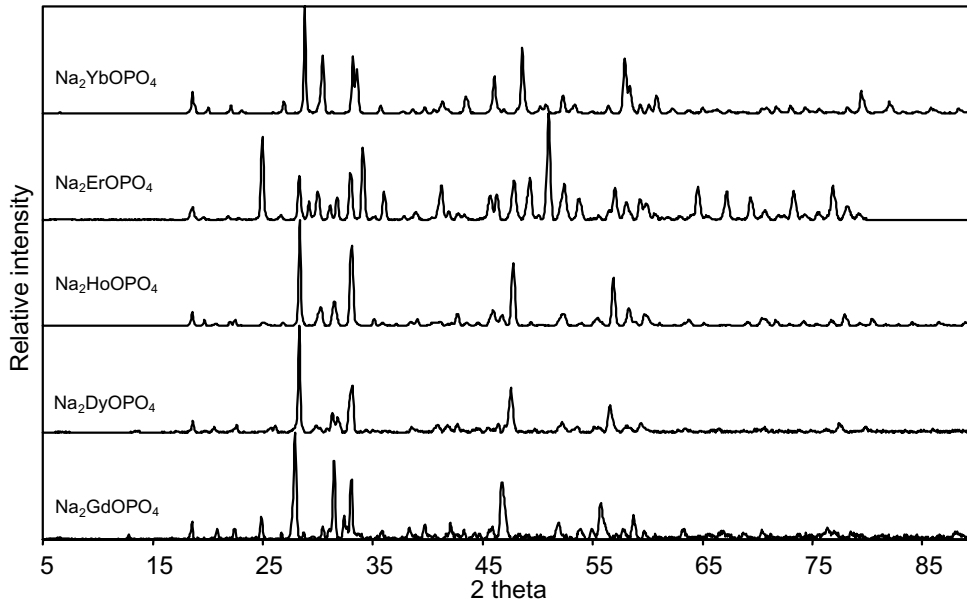


Figure 2. X-ray powder diffraction patterns of set 2.

It is known that Na₂LaOPO₄³⁶ has an orthorhombic structure with the refined unit cell parameters, $a = 13.657(5)$, $b = 11.076(5)$, and $c = 6.7295(3)$ Å. In our study the diffraction peaks of our Na₂LaOPO₄ can be indexed on the basis of an orthorhombic cell with the refined unit cell parameters, $a = 13.60(1)$, $b = 12.71(1)$, and $c = 6.96(1)$ Å, using the CELREF program³⁸ and the probable space group, Pmm2. Table 2 shows the X-ray powder diffraction data of our new Na₂LaOPO₄. The unit cell parameters of previously synthesized sodium lanthanum oxyphosphate and this new phase were similar, but with different cell parameters. The reason is that the former contained Na₃La(PO₄)₂ together with Na₂LaOPO₄. Another reason for the difference is the production temperature. The former was obtained at 1000 °C, while our final product, Na₂LaOPO₄, was heated at 1100 °C.

The unit cell parameters of the other 2 products in set 1, Na₂NdOPO₄ and Na₂SmOPO₄, were indexed in an orthorhombic system with the refined cell parameters of $a = 13.466(5)$, $b = 12.547(6)$, and $c = 6.932(5)$ Å, and $a = 13.54(1)$, $b = 12.577(8)$, and $c = 7.047(5)$ Å, respectively, with the probable space group, Pmm2. Powder diffraction data and hkl values of Na₂LaOPO₄, Na₂NdOPO₄, and Na₂SmOPO₄ are given in Tables 2, 3, and 4, respectively. The calculated hkl values and the XRD data of set 1, in which samples were prepared with the highest temperature (1100 °C), was in accordance with Kizilyalli's work.³⁶ Table 5 summarizes the relationship between the unit cell dimensions of set 1.

Table 2. The X-ray powder diffraction data of Na₂LaOPO₄ (a = 13.60(1), b = 12.71(1), and c = 6.96(1) Å).

d_{obs} (Å)	d_{cal} (Å)	I/I ₀	h k l	d_{obs} (Å)	d_{cal} (Å)	I/I ₀	h k l
6.9642	6.9642	12	0 0 1	1.8993	1.8983	12	6 0 2
4.8307	4.8629	18	2 0 1	1.8772	1.8775	6	6 1 2
4.2873	4.2660	14	3 1 0	1.8329	1.8349	9	4 2 3
4.0009	4.0439	14	1 3 0	1.8294	1.8189	8	6 2 2
3.6671	3.6378	6	3 1 1	1.7730	1.7761	32	5 4 2
3.6157	3.6191	33	0 3 1	1.7263	1.7269	10	1 0 4
3.4048	3.3966	18	4 0 0	1.7187	1.7140	14	0 5 3
3.3482	3.3583	63	0 4 0	1.6952	1.6953	11	7 0 2
3.3115	3.2814	58	4 1 0	1.6780	1.6792	10	0 2 4
3.1951	3.1941	27	2 3 1	1.6667	1.6665	23	1 2 4
3.1400	3.1769	8	0 4 0	1.6515	1.6500	7	8 0 1
3.0506	3.0529	10	4 0 1	1.6327	1.6301	8	2 2 4
2.9956	2.9955	15	4 2 0	1.6156	1.6120	10	3 1 4
2.9520	2.9684	22	4 1 1	1.5951	1.5970	15	8 2 1
2.8687	2.8778	100	2 4 0	1.5727	1.5740	6	7 3 2
2.7485	2.7517	61	4 2 1	1.5534	1.5543	9	1 6 3
2.6573	2.6572	9	5 1 0	1.4890	1.4890	13	7 0 3
2.5266	2.5314	11	5 0 1	1.4209	1.4211	9	4 6 3
2.4926	2.4982	7	1 5 0	1.3573	1.3567	9	2 1 5
2.3719	2.3804	24	2 5 0	1.3488	1.3488	7	6 2 4
2.3363	2.3469	5	0 4 2	1.3454	1.3455	8	5 8 1
2.2960	2.2882	25	1 0 3	1.3176	1.3180	5	4 7 3
2.2440	2.2520	13	1 1 3	1.2957	1.2960	6	7 0 4
2.1741	2.1730	27	5 3 1	1.2926	1.2937	5	10 3 0
2.1493	2.1529	5	1 2 3	1.2896	1.2893	6	7 1 4
2.1300	2.1330	8	6 2 0	1.2539	1.2537	10	2 4 5
2.1110	2.1120	9	3 5 1	1.2435	1.2449	5	1 10 1
2.0562	2.0529	28	0 5 2	1.2226	1.2230	7	4 8 3
2.0192	2.0220	45	2 6 0	1.1830	1.1812	7	6 1 5
1.9918	1.9970	10	6 3 0	1.1747	1.1757	7	9 4 3
1.9653	1.9651	36	2 5 2	1.1472	1.1470	6	2 6 5
1.9356	1.9308	9	4 4 2	1.1305	1.1301	7	10 3 3
1.9106	1.9117	13	5 3 2	1.1289	1.1285	7	10 6 1

Table 3. The X-ray powder diffraction data of $\text{Na}_2\text{NdOPO}_4$ ($a = 13.466(5)$, $b = 12.547(6)$, and $c = 6.932(5)$ Å).

d_{obs} (Å)	d_{cal} (Å)	I/I ₀	h k l	d_{obs} (Å)	d_{cal} (Å)	I/I ₀	h k l
4.8177	4.8310	16	2 0 1	1.6300	1.6276	10	4 4 3
4.2873	4.2256	14	3 1 0	1.6182	1.6173	8	3 0 4
3.9920	3.9854	11	1 3 0	1.6040	1.6040	13	3 1 4
3.6085	3.6085	31	3 1 1	1.6001	1.6010	11	0 3 4
3.3669	3.3669	10	4 0 0	1.5826	1.5827	21	8 2 1
3.2876	3.2513	90	4 1 0	1.5582	1.5576	12	2 3 4
3.2522	3.2432	76	1 1 2	1.5523	1.5541	9	1 8 0
3.1292	3.1292	8	0 4 0	1.5221	1.5230	9	8 3 1
2.9956	2.9933	15	2 1 2	1.4784	1.4788	14	7 0 3
2.9473	2.9428	22	4 1 1	1.4535	1.4528	9	9 1 1
2.8598	2.8522	100	0 4 1	1.4306	1.4319	6	6 4 3
2.8116	2.7966	12	3 3 1	1.4095	1.4085	10	9 3 0
2.7321	2.7263	76	4 2 1	1.4086	1.4070	9	4 6 3
2.5231	2.5132	14	3 2 2	1.3463	1.3467	11	10 0 0
2.3629	2.3546	16	0 5 1	1.3429	1.3426	11	5 6 3
2.2878	2.2893	26	1 4 2	1.3338	1.3334	8	0 6 4
2.2387	2.2226	6	2 5 1	1.2919	1.2917	9	2 3 5
2.1616	2.1684	26	0 2 3	1.2769	1.2757	9	4 1 5
2.1447	2.1409	6	1 2 3	1.2747	1.2747	9	6 6 3
2.0993	2.0971	17	5 1 2	1.2733	1.2732	9	7 5 3
2.0562	2.0552	9	3 0 3	1.2428	1.2405	11	3 9 2
2.0386	2.0414	9	5 4 0	1.2161	1.2159	10	9 6 0
2.0170	2.0211	36	6 2 1	1.2148	1.2139	12	7 8 0
1.9815	1.9767	35	6 3 0	1.2122	1.2117	12	2 10 1
1.9572	1.9583	49	5 4 1	1.1539	1.1545	6	11 0 2
1.9220	1.9239	14	7 0 0	1.1528	1.1518	7	3 9 3
1.8628	1.8632	6	6 1 2	1.1517	1.1516	7	1 0 6
1.8433	1.8436	7	3 3 3	1.1129	1.1127	6	11 3 2
1.7941	1.7922	10	2 4 3	1.1098	1.1101	7	1 3 6
1.7730	1.7733	20	4 6 0	1.1088	1.1079	7	12 0 1
1.7354	1.7372	18	5 1 3	1.1078	1.1076	8	2 11 1
1.6837	1.6834	23	8 0 0	1.1073	1.1073	7	7 2 5
1.6695	1.6684	9	8 1 0	1.1058	1.1062	8	5 5 5
1.6667	1.6673	10	7 1 2	1.1048	1.1047	8	12 2 0
1.6570	1.6581	13	1 2 4	1.1034	1.1036	7	12 1 1
1.6434	1.6467	8	2 5 3				

Table 4. The X-ray powder diffraction data of Na₂SmOPO₄ (a = 13.54(1), b = 12.577(8), and c = 7.047(5) Å) (intensities over 10 are given).

d_{obs} (Å)	d_{cal} (Å)	I/I ₀	h k l	d_{obs} (Å)	d_{cal} (Å)	I/I ₀	h k l
4.3391	4.2482	10	3 1 0	1.6065	1.6038	22	7 4 1
4.0277	3.9998	11	1 3 0	1.5826	1.5854	29	4 7 0
3.6375	3.6375	29	3 1 1	1.5582	1.5595	18	1 8 0
3.3857	3.3857	12	4 0 0	1.5347	1.5348	14	6 6 0
3.2876	3.2888	91	1 1 2	1.5131	1.5145	15	8 1 2
3.2522	3.2514	86	3 2 1	1.4773	1.4764	17	3 6 3
3.1508	3.1400	15	0 4 0	1.4219	1.4208	12	7 6 0
2.9956	2.9951	16	1 2 2	1.4133	1.4101	12	2 5 4
2.9378	2.9651	32	4 1 1	1.4095	1.4084	11	0 0 5
2.8732	2.8678	100	0 4 1	1.4067	1.4070	10	6 6 2
2.8030	2.8056	16	1 4 1	1.4048	1.4045	10	6 7 0
2.7444	2.7445	94	4 2 1	1.4011	1.4008	10	1 0 5
2.7120	2.7109	28	3 1 2	1.3766	1.3767	12	5 7 2
2.3719	2.3659	19	0 5 1	1.3721	1.3723	10	8 4 2
2.2906	2.3023	34	4 4 0	1.3463	1.3465	16	10 1 0
2.1666	2.1641	30	5 3 1	1.3446	1.3445	16	3 0 5
2.1087	2.1084	16	4 3 2	1.3429	1.3418	14	2 9 1
2.0924	2.0933	11	0 6 0	1.3338	1.3337	12	5 8 1
2.0878	2.0912	13	2 2 3	1.3313	1.3325	14	9 4 1
2.0429	2.0449	15	0 5 2	1.3280	1.3284	17	1 3 5
2.0064	2.0065	65	0 6 1	1.2889	1.2889	14	6 8 0
1.9713	1.9691	68	5 4 1	1.2814	1.2814	12	2 8 3
1.9632	1.9598	78	2 3 3	1.2733	1.2733	10	4 2 5
1.9454	1.9393	30	4 5 1	1.2631	1.2625	12	2 4 5
1.9125	1.9121	23	7 1 0	1.2617	1.2615	10	5 7 3
1.8808	1.8800	17	0 4 3	1.2129	1.2129	10	8 7 1
1.8754	1.8788	11	6 1 2	1.2116	1.2115	12	4 9 2
1.8663	1.8656	10	7 0 1	1.2090	1.2087	14	2 5 5
1.8433	1.8440	17	4 2 3	1.2014	1.2014	13	4 4 5
1.8398	1.8418	12	5 5 0	1.1989	1.1995	12	0 9 3
1.8329	1.8328	10	6 4 0	1.1915	1.1921	11	10 5 0
1.7778	1.7787	22	1 7 0	1.1897	1.1895	11	6 1 5
1.7746	1.7739	24	5 0 3	1.1434	1.1439	10	9 0 4
1.7217	1.7245	39	1 7 1	1.1423	1.1428	10	11 2 2
1.6851	1.6841	24	2 7 1	1.0970	1.0972	14	12 2 1
1.6612	1.6625	32	2 5 3	1.0960	1.0958	10	1 4 6
1.6584	1.6563	33	5 6 0	1.0951	1.0957	12	9 7 2
1.6327	1.6331	18	6 5 1	1.0941	1.0941	13	8 8 2
1.6195	1.6225	16	3 7 1				

Table 5. The unit cell parameters of set 1.

(Å)	Na ₂ LaOPO ₄	Na ₂ NdOPO ₄	Na ₂ SmOPO ₄
a	13.60 (1)	13.466 (5)	13.54 (1)
b	12.71 (1)	12.547 (6)	12.577 (8)
c	6.96 (1)	6.932 (5)	7.047 (5)

The most intense peaks were observed at $d = 2.8687$, 2.8598 , and 2.8732 Å for Na₂LaOPO₄, Na₂NdOPO₄, and Na₂SmOPO₄, respectively. Furthermore, the splitting of peaks was observed at $d = 3.45$ and 3.55 Å, $d = 3.29$ and 3.25 Å, and $d = 3.29$ and 3.25 Å, respectively, while this splitting was observed at 3.27 and 3.23 Å in the data of the lanthanum compound.³⁶

In the second set, Na₂DyOPO₄, Na₂HoOPO₄, Na₂ErOPO₄, and Na₂YbOPO₄ were synthesized for the first time at 1100 °C. The new phase of Na₂GdOPO₄ was also obtained from a solid state reaction at the same temperature. The X-ray powder diffraction patterns are given in Figure 2. The indexing of the data showed that Na₂GdOPO₄ and the new products are also orthorhombic, with the unit cell parameters, $a = 13.37(1)$, $b = 12.775(9)$, and $c = 6.910$ Å (9), $a = 13.66(2)$, $b = 12.609(9)$, and $c = 6.611(6)$ Å, $a = 13.148(4)$, $b = 12.577(2)$, and $c = 6.967(1)$ Å, $a = 13.563(5)$, $b = 12.604(4)$, and $c = 7.003(3)$ Å, and $a = 13.501(7)$, $b = 17.579(9)$, $c = 6.729(4)$ Å for Na₂DyOPO₄, Na₂HoOPO₄, Na₂ErOPO₄, and Na₂YbOPO₄, respectively, with the probable space group of Pmm2 for this set. The hkl indices and d splitting values are given in Tables 6-10.

Table 11 represents the unit cell parameters of set 2, in which there are similarities among the set, except for Yb, which has $b = 17.579(9)$ Å. Similar hkl values were observed in all products. Examination of the hkl indices and unit cell parameters showed that there are some resemblances between these products and Na₂LnOPO₄-type orthorhombic compounds, where Ln = La, Nd, and Sm. The splitting of the peak around $d = 3.45$ and 3.25 Å was not observed in these products.

FTIR and Raman Studies

The IR and Raman spectra of set 1 are given in Figures 3, and 4, respectively. Figures 5 and 6 show the IR and Raman spectra of set 2, respectively. According to Kizilyalli,³⁷ ν_{as} and ν_s bands, assigned as ν_3 (F2) were observed between 1136 , 1099 , 1034 , 982 , 965 , and 945 cm⁻¹. Tables 12 and 13 indicate the IR and Raman data of both sets and assignments, respectively. Table 12 shows that ν_3 (F2) bands were between 1084 - 1099 , 1030 - 1053 , 976 - 982 , 957 - 971 , and 945 - 954 cm⁻¹ for both sets, respectively. Kizilyalli³⁷ also indicated that the bands at 926 and 909 cm⁻¹ are due to stretching modes assigned as ν_1 (A1), which were observed in our samples at band 913 cm⁻¹ and bands 921 - 926 cm⁻¹. She also stated that the bands around 604 , 579 , 560 , 548 , 523 , and 470 cm⁻¹ are ascribed to the δ (O-P-O), which is assigned as ν_4 (F2). These bands were present at 598 - 605 , 574 - 579 , 559 - 565 , 541 - 551 , 523 - 526 , 468 - 472 , and 403 - 409 cm⁻¹ for both sets, respectively. Finally, bands at 406 , 381 , and 367 cm⁻¹ are attributed to deformation modes and are assigned as ν_3 (E) according to Kizilyalli.³⁷ In the IR table of the both sets, the bands around 403 - 409 cm⁻¹ are obvious. Some of these bands were observed in Raman spectra of the products.

Table 6. The X-ray powder diffraction data of Na₂GdOPO₄ (a = 13.37(1), b = 12.775(9), and c = 6.910(9) Å).

d_{obs} (Å)	d_{cal} (Å)	I/I ₀	h k l	d_{obs} (Å)	d_{cal} (Å)	I/I ₀	h k l
6.9100	6.9100	5	0 0 1	1.5244	1.5237	6	4 1 4
4.7791	4.8043	17	2 0 1	1.4710	1.4701	10	7 0 3
4.2568	4.2601	11	0 3 0	1.4690	1.4694	10	3 8 1
3.9656	4.0590	11	1 3 0	1.4669	1.4643	11	8 2 2
3.5799	3.5925	22	2 3 0	1.4627	1.4605	6	7 1 3
3.3420	3.3420	7	4 0 0	1.4415	1.4416	5	1 8 2
3.1951	3.1951	100	0 4 0	1.4277	1.4308	5	0 7 3
2.9331	2.9286	12	4 1 1	1.4238	1.4231	6	1 5 4
2.8777	2.8827	10	2 4 0	1.4200	1.4200	6	0 9 0
2.8377	2.8341	74	1 4 1	1.4171	1.4171	5	2 8 2
2.7650	2.7667	23	2 2 2	1.4058	1.4063	7	6 6 2
2.7403	2.7304	12	3 0 2	1.4011	1.4025	8	9 3 0
2.7080	2.7220	56	4 2 1	1.3965	1.3987	9	8 5 0
2.6383	2.6310	6	1 3 2	1.3891	1.3897	6	7 3 3
2.5129	2.5108	7	3 2 2	1.3846	1.3836	5	6 7 1
2.5061	2.4935	9	5 0 1	1.3651	1.3652	7	6 0 4
2.3480	2.3458	11	0 4 2	1.3608	1.3610	6	8 4 2
2.3161	2.3105	5	1 4 2	1.3362	1.3368	10	10 0 0
2.2657	2.2646	14	5 3 0	1.3346	1.3345	8	9 2 2
2.1641	2.1669	6	0 2 3	1.3232	1.3233	6	8 2 3
2.1469	2.1467	16	2 1 3	1.2851	1.2856	6	10 2 1
2.1348	2.1301	7	0 6 0	1.2821	1.2811	6	7 0 4
2.1228	2.1205	5	6 0 1	1.2740	1.2744	7	7 5 3
2.1110	2.1112	5	3 5 1	1.2711	1.2722	5	4 1 5
2.0901	2.0919	9	6 1 1	1.2689	1.2684	5	0 4 5
2.0429	2.0462	7	3 0 3	1.2667	1.2628	5	1 4 5
2.0234	2.0262	6	0 3 3	1.2546	1.2548	5	0 7 4
1.9877	2.0033	9	1 3 3	1.2525	1.2524	6	4 2 5
1.9774	1.9743	13	6 3 0	1.2497	1.2493	7	1 7 4
1.9434	1.9472	54	2 6 1	1.2462	1.2462	12	2 4 5
1.8919	1.8940	5	5 3 2	1.2407	1.2409	7	10 1 2
1.8808	1.8760	6	4 1 3	1.2373	1.2351	9	2 10 1
1.8503	1.8505	5	1 4 3	1.2326	1.2327	7	8 7 0
1.8260	1.8258	5	0 7 0	1.2180	1.2184	8	9 6 0
1.7602	1.7612	16	2 7 0	1.2142	1.2140	7	10 4 1
1.7083	1.7067	6	2 7 1	1.2103	1.2107	6	1 5 5
1.6995	1.6981	11	1 1 4	1.2039	1.2039	5	6 7 3
1.6723	1.6726	11	2 0 4	1.1824	1.1804	5	8 2 4

Table 6. Continued.

d_{obs} (Å)	d_{cal} (Å)	I/I ₀	h k l	d_{obs} (Å)	d_{cal} (Å)	I/I ₀	h k l
1.6488	1.6548	34	1 2 4	1.1776	1.1765	5	11 2 1
1.6393	1.6392	17	7 4 0	1.1752	1.1748	5	4 7 4
1.6078	1.6107	6	3 0 4	1.1579	1.1575	5	3 10 2
1.5951	1.5950	10	7 4 1	1.1556	1.1560	5	8 3 4
1.5913	1.5937	10	4 6 2	1.1456	1.1458	5	0 11 1
1.5875	1.5890	5	6 1 3	1.1103	1.1108	6	3 1 6
1.5838	1.5863	5	1 8 0	1.1093	1.1092	8	9 2 4
1.5703	1.5691	24	2 7 2	1.1073	1.1070	8	11 3 2
1.5475	1.5533	9	1 6 3	1.0917	1.0930	5	9 7 2
1.5452	1.5460	7	1 8 1				

Table 7. The X-ray powder diffraction data of Na₂DyOPO₄ (a = 13.66(2), b = 12.609(9), and c = 6.611(6) Å).

d_{obs} (Å)	d_{cal} (Å)	I/I ₀	h k l	d_{obs} (Å)	d_{cal} (Å)	I/I ₀	h k l
4.7663	4.7663	12	2 0 1	1.6543	1.6539	6	1 5 3
4.3182	4.3401	6	1 2 1	1.6247	1.6254	27	7 2 2
3.9310	4.0151	9	1 3 0	1.5938	1.5936	5	5 3 3
3.4112	3.4112	7	4 0 0	1.5888	1.5888	7	6 0 3
3.1508	3.1508	100	0 4 0	1.5850	1.5839	7	0 7 2
3.0005	2.9999	8	4 2 0	1.5534	1.5520	10	3 1 4
2.8553	2.8605	19	2 4 0	1.4658	1.4656	5	3 3 4
2.8159	2.8002	15	3 3 1	1.4048	1.4008	5	3 4 4
2.7037	2.7001	45	2 2 2	1.3471	1.3479	5	9 2 2
2.2228	2.2206	5	0 0 3	1.3437	1.3436	5	6 0 4
2.2046	2.2047	8	3 5 0	1.3321	1.3323	6	0 0 5
2.1616	2.1644	8	5 3 1	1.2846	1.2849	5	0 8 3
2.1493	2.1522	6	6 0 1	1.2476	1.2485	5	2 3 5
2.1157	2.1115	9	2 0 3	1.2346	1.2345	5	11 1 0
2.0386	2.0367	5	6 2 1	1.2319	1.2333	10	1 10 1
2.0234	2.0272	5	4 5 0	1.2306	1.2306	9	10 4 1
1.9960	1.9954	6	3 0 3	1.2279	1.2281	7	9 2 3
1 9553	1 9493	9	7 0 0	1.2021	1.2024	5	4 8 3
1.9317	1.9280	8	2 5 2	1.2008	1.2000	6	10 5 0
1.9087	1.9070	43	3 6 0	1.9996	1.9999	6	9 3 3
1.7508	1.7537	11	5 4 2	1.0965	1.0961	5	0 10 3
1.7083	1.7090	7	7 3 1	1.0941	1.0934	6	0 2 6
1.7054	1.7056	7	8 0 0	1.0926	1.0926	5	1 10 3
1.6653	1.6654	6	0 0 4				

Table 8. The X-ray powder diffraction data of $\text{Na}_2\text{HoOPO}_4$ ($a = 13.148(4)$, $b = 12.577(2)$, and $c = 6.967(1)$ Å).

d_{obs} (Å)	d_{cal} (Å)	I/I ₀	h k l	d_{obs} (Å)	d_{cal} (Å)	I/I ₀	h k l
4.7791	4.7790	14	2 0 1	1.6169	1.6163	46	3 0 4
4.5139	4.5464	6	2 2 0	1.5813	1.5804	18	6 1 3
4.0277	4.1410	5	3 1 0	1.5475	1.5444	12	1 6 3
3.9569	3.9957	6	1 3 0	1.4576	1.4573	7	8 4 0
3.1454	3.1454	100	0 4 0	1.3590	1.3582	5	0 2 5
2.9473	2.9651	18	1 2 2	1.3362	1.3385	8	0 6 4
2.8377	2.8377	24	2 4 0	1.3160	1.3156	6	10 0 0
2.7080	2.6882	77	4 2 1	1.2769	1.2769	5	7 7 1
2.5544	2.5559	8	3 4 0	1.2414	1.2397	6	4 6 4
2.3046	2.2969	7	1 4 2	1.2394	1.2387	5	9 4 2
2.1134	2.0983	12	5 0 2	1.2380	1.2381	4	0 10 1
1.9733	1.9844	15	6 2 1	1.2253	1.2252	12	4 3 5
1.9414	1.9431	11	6 3 0	1.1940	1.1948	8	8 0 4
1.9031	1.9027	60	4 4 2	1.1903	1.1906	6	11 1 0
1.7493	1.7455	12	5 4 2	1.1245	1.1245	5	1 11 1
1.6556	1.6534	9	7 0 2				

Table 9. The X-ray powder diffraction data of $\text{Na}_2\text{ErOPO}_4$ ($a = 13.563(5)$, $b = 12.604(4)$, and $c = 7.003(3)$ Å).

d_{obs} (Å)	d_{cal} (Å)	I/I ₀	h k l	d_{obs} (Å)	d_{cal} (Å)	I/I ₀	h k l
4.7537	4.6837	12	0 2 1	1.7446	1.7437	34	0 7 1
3.5658	3.5726	78	2 3 0	1.7025	1.7041	21	5 2 3
3.1508	3.1508	41	0 4 0	1.6130	1.6156	31	0 3 4
3.0557	3.0548	17	4 0 1	1.5888	1.5901	17	1 7 2
2.9809	2.9852	27	1 2 2	1.5558	1.5557	20	4 0 4
2.8732	2.8732	14	0 4 1	1.5267	1.5272	7	1 8 1
2.8159	2.8187	21	3 3 1	1.4425	1.4440	31	6 4 3
2.7160	2.7160	44	5 0 0	1.3939	1.3917	27	9 3 1
2.6270	2.6280	68	1 3 2	1.3529	1.3523	21	9 2 2
2.4926	2.4942	27	5 2 0	1.3313	1.3330	10	5 4 4
2.3132	2.3120	8	3 3 2	1.2904	1.2890	28	3 6 4
2.1892	2.1884	33	0 2 3	1.2588	1.2585	8	8 4 3
1.9836	1.9902	23	1 6 1	1.2567	1.2550	7	0 7 4
1.9612	1.9586	25	2 5 2	1.2394	1.2392	32	2 10 0
1.8993	1.9006	37	6 0 2	1.2213	1.2209	14	5 2 5
1.8468	1.8476	40	5 5 0	1.2084	1.2094	7	3 7 4
1.7892	1.7864	100	5 5 1	1.2065	1.2062	6	6 7 3

Table 10. The X-ray powder diffraction data of $\text{Na}_2\text{YbOPO}_4$ ($a = 13.501(7)$, $b = 17.579(9)$, and $c = 6.729(4)$ Å).

d_{obs} (Å)	d_{cal} (Å)	I/I ₀	h k l	d_{obs} (Å)	d_{cal} (Å)	I/I ₀	h k l
4.7663	4.7663	20	2 0 1	1.6300	1.6300	7	8 1 1
4.4357	4.4256	6	2 3 0	1.5913	1.5913	52	3 10 1
4.0187	4.0058	7	3 2 0	1.5801	1.5818	27	3 9 2
3.3055	3.3055	11	0 1 2	1.5558	1.5554	9	2 11 0
3.0973	3.1169	100	0 5 1	1.5392	1.5408	9	5 9 1
2.9331	2.9305	55	0 6 0	1.5221	1.5221	17	3 3 4
2.7001	2.7001	54	5 0 0	1.4912	1.4917	5	7 7 1
2.6688	2.6688	42	5 1 0	1.4336	1.4323	6	5 9 2
2.5129	2.5119	8	0 7 0	1.3362	1.3361	5	0 8 4
2.3276	2.3832	5	1 7 1	1.3297	1.3296	6	1 8 4
2.2684	2.2876	6	2 5 2	1.3152	1.3156	7	10 3 0
2.1816	2.1810	12	1 6 2	1.2949	1.2953	8	3 13 0
2.0809	2.0854	16	3 7 1	1.2755	1.2758	6	7 10 1
1.9693	1.9728	36	4 5 2	1.2567	1.2572	5	0 5 5
1.9336	1.9335	4	1 9 0	1.2220	1.2218	6	1 12 3
1.8718	1.8732	62	1 5 3	1.2052	1.2050	22	10 4 2
1.8158	1.8142	7	7 2 1	1.1741	1.1736	12	3 10 4
1.7974	1.7921	9	3 9 0	1.1315	1.1317	6	2 8 5
1.7477	1.7437	17	3 5 3	1.1063	1.1064	5	8 12 0
1.7158	1.7174	9	5 1 3				

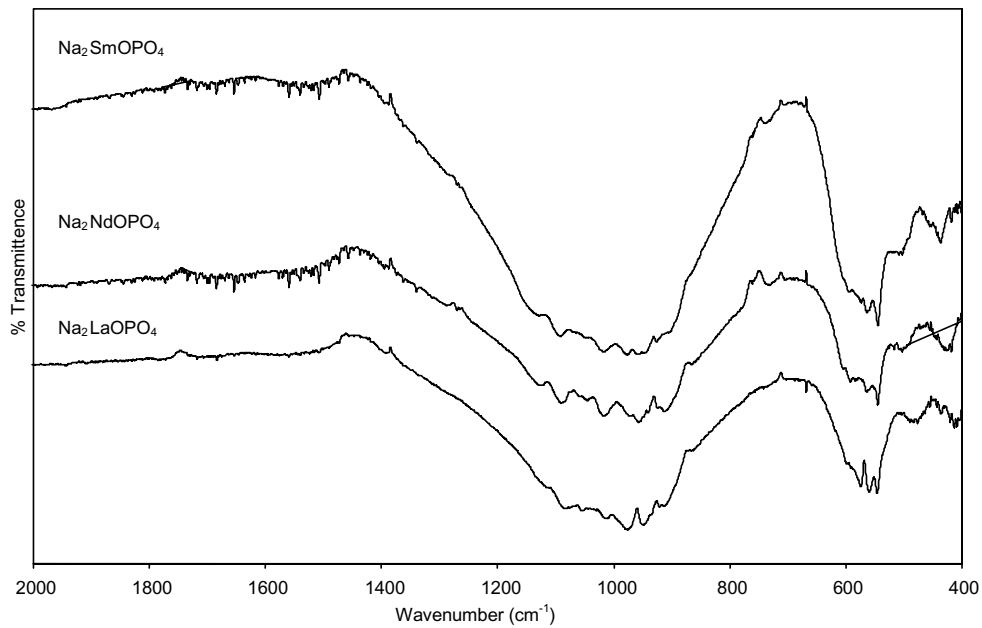
**Figure 3.** FT-IR spectra of set 1.

Table 11. The unit cell parameters of set 2.

(Å)	Na ₂ GdOPO ₄	Na ₂ DyOPO ₄	Na ₂ HoOPO ₄	Na ₂ ErOPO ₄	Na ₂ YbOPO ₄
a	13.37 (1)	13.66 (2)	13.148 (4)	13.563 (5)	13.501 (7)
b	12.775 (9)	12.609 (9)	12.577 (2)	12.604 (4)	17.579 (9)
c	6.910 (9)	6.611 (6)	6.967 (1)	7.003 (3)	6.729 (4)

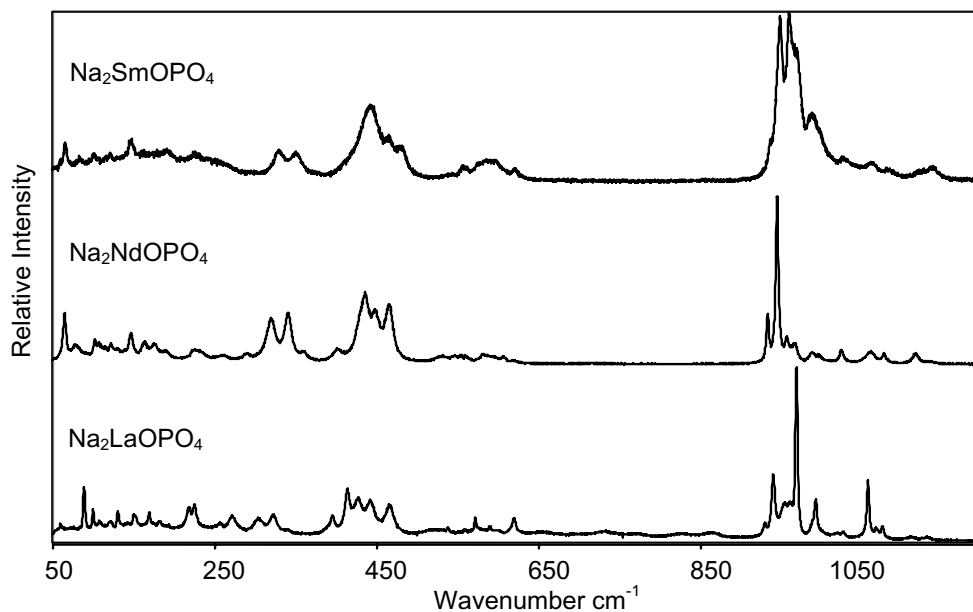


Figure 4. Raman spectra of set 1.

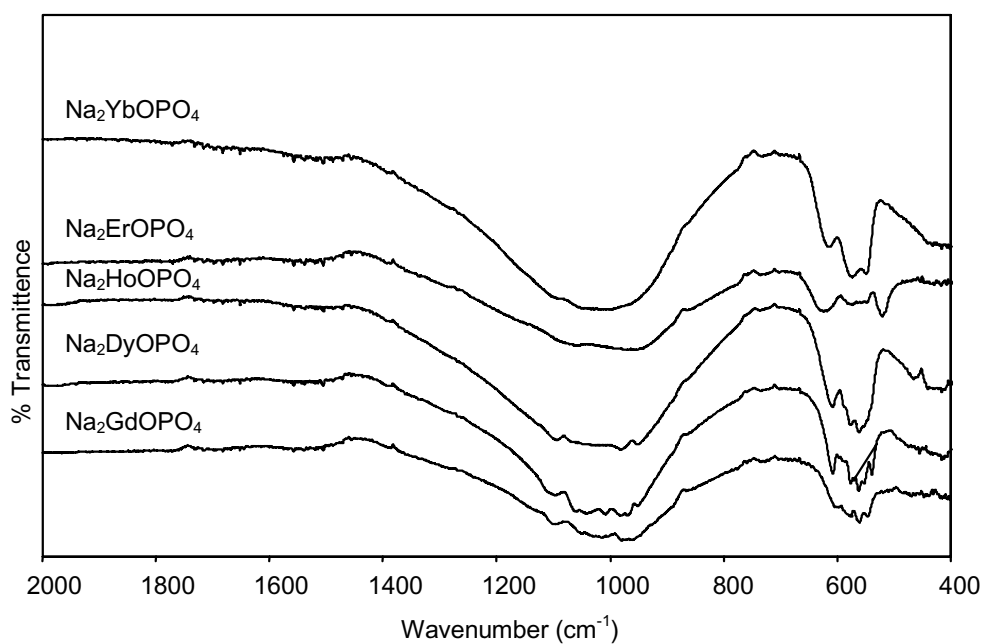


Figure 5. FT-IR spectra of set 2.

Table 12. IR band locations for the products (cm^{-1}).

Assignments	$\text{Na}_2\text{LaOPO}_4$	$\text{Na}_2\text{NdOPO}_4$	$\text{Na}_2\text{SmOPO}_4$	$\text{Na}_2\text{GdOPO}_4$	$\text{Na}_2\text{DyOPO}_4$	$\text{Na}_2\text{HoOPO}_4$	$\text{Na}_2\text{ErOPO}_4$	$\text{Na}_2\text{YbOPO}_4$
ν_3	1084	1090	1136	1099	1098	1095		
	1053	1044	1092	1030	1044		1036	
	976		978	982	982	982	978	
		957	957	963	971		957	
	950	941	945		953	954		
ν_1	921	924	926				926	
	913	913						
	599	605		602	599		598	
ν_4	574		574	577	579	579	576	576
	560	564	564	561	565	559	559	
	547	546	545	548	541		551	551
		526	523	526	520	523	523	523
	472	472	468	471	477	472	472	468
ν_2	409	403	408	405	409	406	408	408

Table 13. The Raman data of the products (cm^{-1}).

Assignment	$\text{Na}_2\text{LaOPO}_4$	$\text{Na}_2\text{NdOPO}_4$	$\text{Na}_2\text{SmOPO}_4$	$\text{Na}_2\text{GdOPO}_4$	$\text{Na}_2\text{DyOPO}_4$	$\text{Na}_2\text{HoOPO}_4$	$\text{Na}_2\text{ErOPO}_4$	$\text{Na}_2\text{YbOPO}_4$
ν_3			1153		1135		1108	
		1023			1031		1030	
	977				977			
	964	955	958	965	958	932	949	
		944			944			
ν_1		932			927			
	625					609	608	
ν_4	574		585					
							561	569
	574						525	
	468	464		464			472	

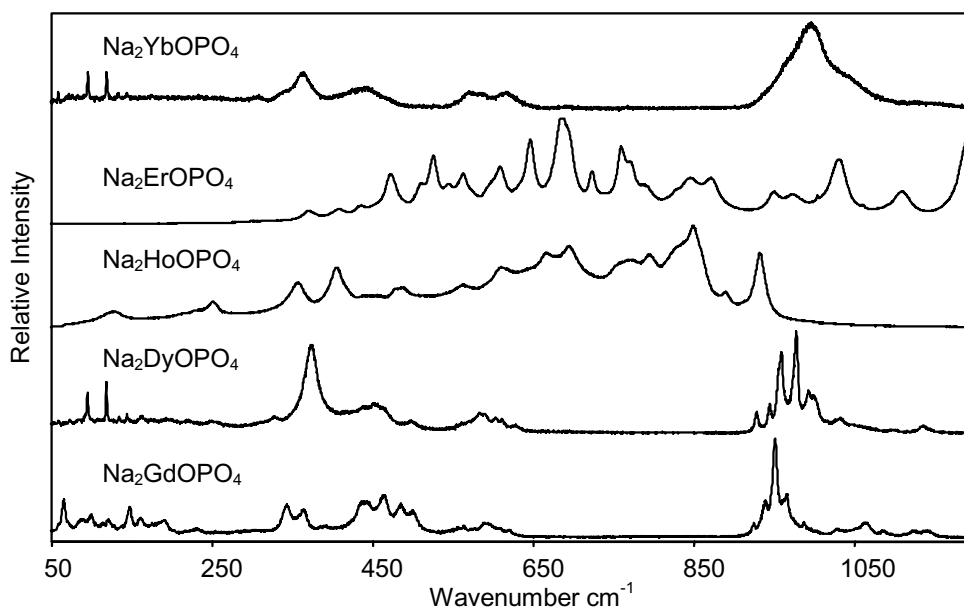


Figure 6. Raman spectra of set 2.

The presence of the tetrahedral PO_4 ion with T_d symmetry is obvious since the T_d symmetry has 4 internal modes of vibration, $\nu_1 = 938 \text{ cm}^{-1}$ (R), $\nu_2 = 420 \text{ cm}^{-1}$ (R), $\nu_3 = 1017 \text{ cm}^{-1}$ (IR, R), and $\nu_4 = 567 \text{ cm}^{-1}$ (IR, R).³⁷ Kızılyallı³⁷ also mentioned that the antisymmetric stretching modes are found between 1290 and 1050 cm^{-1} , and the symmetric modes between 1050 and 900 cm^{-1} . In our results these bands were also present. Hudson³⁹ and Nakamoto⁴⁰ stated that the highest frequency observed is due to antisymmetric stretching involving the terminal bond, a bond between a phosphorus atom and a so-called unshared oxygen atom or the shortest bond. For instance, in $\text{KTiOPO}_4 \nu_{as}\text{P-O}$ was observed around 1135 cm^{-1} . According to Kızılyallı,³⁷ stretching modes were observed at bands 926 and 909 cm^{-1} , which we observed at band 913 cm^{-1} and at bands 921-926 cm^{-1} . The bands between 604 and 470 are fundamental for $\delta(\text{O-P-O})$ bands, which were 605 and 478 cm^{-1} in the present study. Finally, our samples have deformation modes between 406 and 367 cm^{-1} . The products have bands around 403-409 cm^{-1} and since FTIR instrumentation can detect peaks only up to 400 cm^{-1} , the other deformation peaks are not present. These results confirmed that our samples have a KTP-related $\text{Na}_2\text{GdOPO}_4$ structure.

SEM Studies

The particle morphology of both sets of specimens was investigated using SEM, as given in Figure 7. These SEM observations showed that some uniformity exists in the shape and particle size of the specimens in both sets. In Figure 7a ($\text{Na}_2\text{LaOPO}_4$) it can easily be detected that small particles are around $1 \mu\text{m}$ and the large particles are around 5-10 μm . It is also obvious that in Figure 7b ($\text{Na}_2\text{NdOPO}_4$) there is a large particle in the middle of the micrograph, similar to the large particles in Figure 7c ($\text{Na}_2\text{SmOPO}_4$) and 7d ($\text{Na}_2\text{GdOPO}_4$). Yet, in Figure 7e ($\text{Na}_2\text{DyOPO}_4$) and 7f ($\text{Na}_2\text{HoOPO}_4$) the particles are smaller and more homogeneous than those in Figure 7b ($\text{Na}_2\text{NdOPO}_4$). In Figure 7g ($\text{Na}_2\text{YbOPO}_4$) there are small and large particles present in the micrograph; therefore, among these products, particle size can be given as between 1 and 10 μm .

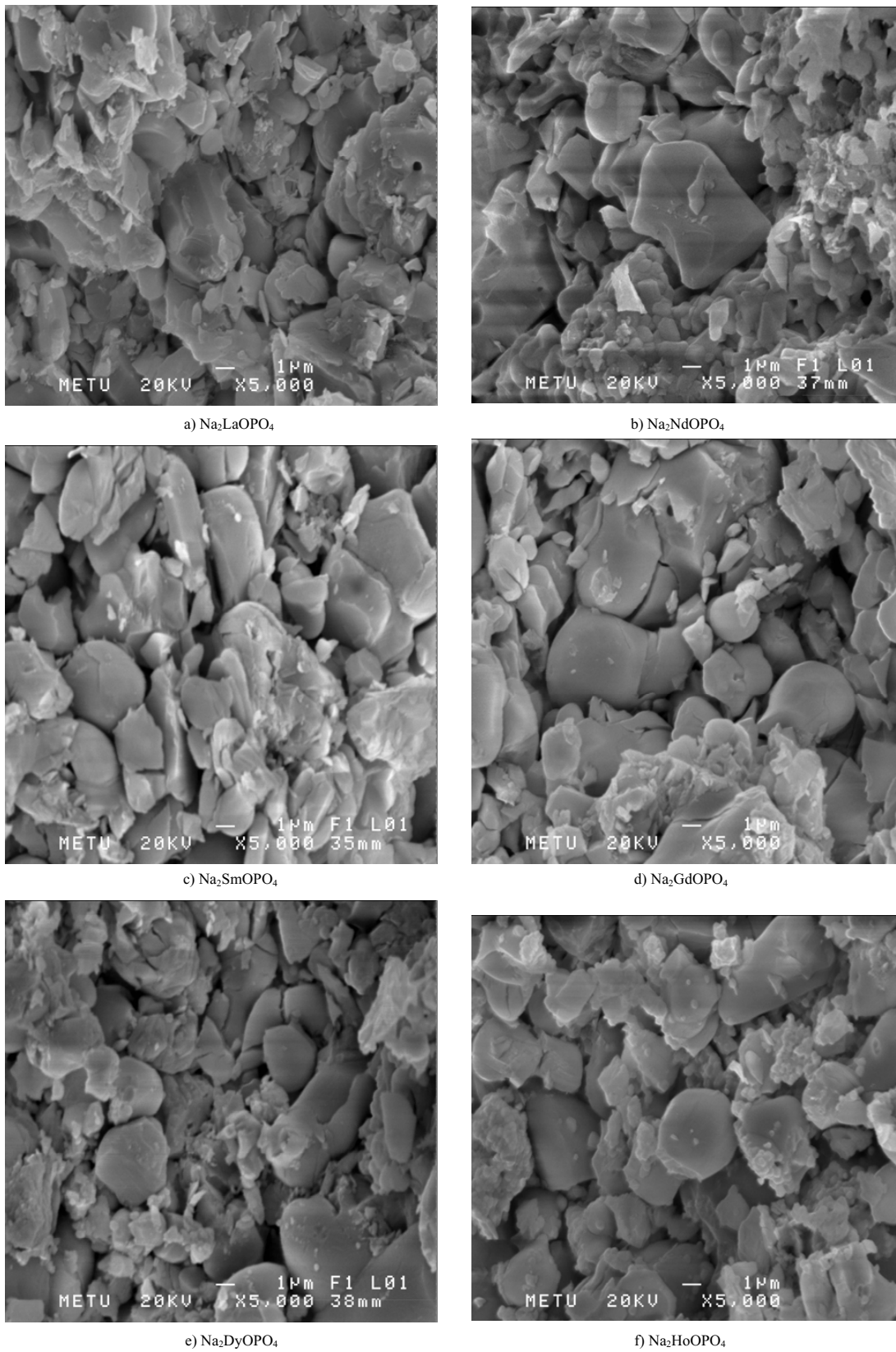
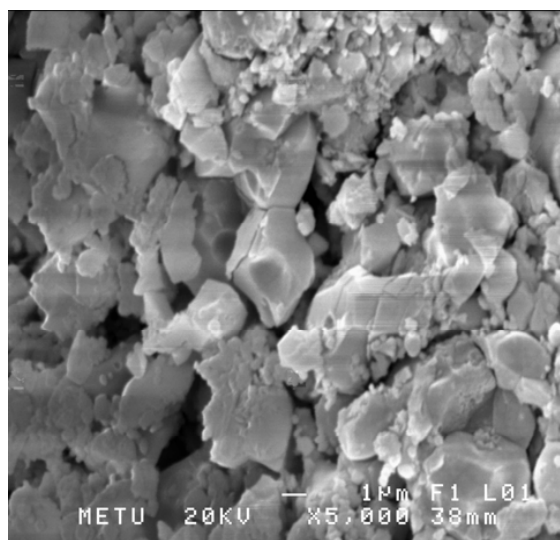


Figure 7. SEM micrographs of the products.



g) Na₂YbOPO₄

Figure 7. Continued.

Conclusion

Na₂GdOPO₄ (sodium gadolinium oxyphosphate) and Na₂LaOPO₄ (sodium lanthanum oxyphosphate) were synthesized from solid state reactions, respectively, and indexed in the orthorhombic system with the probable space group, Pmm2. Their flux growth process failed and single crystals could not be obtained.

In the present study 2 sets of new sodium rare earth oxyphosphates were synthesized at 1100 °C, firstly by the solid state reaction method from Ln₂O₃ (where Ln = La, Nd, Sm, Gd, Dy, Ho, Er, and Yb), Na₂CO₃, and NH₄H₂PO₄. In the first set of compounds, Na₂LaOPO₄, Na₂NdOPO₄, and Na₂SmOPO₄ have the unit cell parameters, a = 13.60(1), b = 12.71(1), and c = 6.96(1) Å, a = 13.466(5), b = 12.547(6), and c = 6.932(5) Å, and a = 13.54(1), b = 12.577(8), c = 7.047(5) Å, respectively, with the probable space group, Pmm2. The splitting of the peaks in the x-ray powder diffraction patterns was observed in all compounds in set 1 at d = 3.45 and 3.55 Å, d = 3.29 and 3.25 Å, and d = 3.29, and 3.25 Å, respectively.

Furthermore with the help of the same procedure new orthorhombics, Na₂DyOPO₄, Na₂HoOPO₄, Na₂ErOPO₄, and Na₂YbOPO₄ were synthesized at 1100 °C for the first time. However, splitting of powder X-ray diffraction peaks were not observed throughout set 2.

All products show the characteristic MTiOPO₄-type compounds, except for the Ti-O bands in the IR spectrum of both sets. Yet, in the Raman data some of the characteristic peaks were observed in all samples. Some coincidences in IR and Raman spectra of both sets were found.

Scanning electron micrographs of set 1 are similar to each other and to set 2, with particles between 1 and 10 µm.

Acknowledgement

This work was supported by BAP-2005-07-02-00-53. The authors also dedicate this paper to the memory of Professor Dr. Meral Kizilyalli.

References

1. A. Miyamoto, Y. Mori, Y. Okada, T. Sasaki and S. Nakai, **J. Crystal Growth** 156, 303-306, (1995).
2. L. Moreno-Real, E.R. Losilla, M.A.G. Aranda, M. Martinez-Lara, S. Bruque and M. Gabas, **J. Solid State Chem.** 137, 289-294, (1998).
3. M. Ketatani, F. Abraham and O. Mentre, **Solid State Sciences** 1, 449-460, (1999).
4. L. Griesel, J.K. Bartley, R.P.K. Wells and G.J. Hutchings, **J. Molecular Catalysis A: Chemical** 220, 113-119, (2004).
5. A. Mizrahi, J.P. Wignacourt and H. Steinfink, **J. Solid State Chem.** 133, 516-521, (1997).
6. E.M. Ketatni, M. Huve, F. Abraham and O. Mentre, **J. Solid State Chem.** 172, 327-338, (2003).
7. I. Bhamuik, S.G. Moorthy, R. Bhatt, R. Sundar, A.K. Karnali and V.K. Wadhawan, **J. Crystal Growth** 243, 522-525, (2002).
8. A.E. Jazouli, S. Krimi, B. Manoun, J.P. Chaminade, P. Graverau and D.D. Waal, **Ann. Chim. Sci. Mat.** 23, 7-10, (1998).
9. V.I. Chani, K. Shimamura, S. Endo and T. Fukuda, **J. Crystal Growth** 173, 117-122, (1997).
10. J. Koseva, V. Nikolov and P. Peshev, **J. Alloys and Compounds** 353, L1-L4, (2003).
11. S.G. Moorthy, F.J. Kumar, C. Subramanian, G. Bocelli and P. Ramasamy, **Materials Letters** 36, 266-270, (1998).
12. R. Sole, X. Ruiz, R. Cabre, J. Gavalda, M. Aguilo, F. Diaz, V. Nikolov and X. Solans, **J. Crystal Growth** 167, 681-685, (1996).
13. V.I. Chani, K. Shimamura, S. Endo and T. Fukuda, **J. Crystal Growth** 169, 604-605, (1996).
14. V.I. Chani and T. Fukuda, **J. Crystal Growth** 206, 245-248, (1999).
15. J.J. Carvajal, V. Nikolov, R. Sole, J. Gavalda, J. Massons, M. Aguilo and F. Diaz, **Chem. Mater.** 14, 3136-3142, (2002).
16. J.J. Carvajal, R. Sole, J. Gavalda, J. Massons, M. Aguilo and F. Diaz, **Crystal Growth & Design** 1 (6), 479-484, (2001).
17. X.B. Hu, H. Liu, J.Y. Wang, H.J. Zhang, H.D. Jiang, S.S. Jiang, Q. Li, Y.L. Tian, Y.Y. Huang, W.X. Huang and W. He, **Optical Materials** 23, 369-372, (2003).
18. X. Wang, X. Yuan, W. Li, J. Qi, S. Wang and D. Shen, **J. Crystal Growth** 237-239 (1), 672-675, (2002).
19. J. Zhang, J. Wang, B. Ge, Y. Liu, X. Hu and R.I. Boughton, **J. Crystal Growth** 267, 517-521, (2004).
20. A. Kling, M. Rico, C. Zaldo, M. Aguilo and F. Diaz **Nuclear Instruments and Methods in Physics Research B** 218, 271-276, (2004).
21. C. Zaldo, M. Rico, F. Diaz and J.J. Carvajal, **Optical Materials** 13, 175-180, (1999).
22. C. Zaldo, M.J. Martin and F. Diaz, **Materials Letters** 45, 107-110, (2000).
23. C. Zaldo, M. Rico, M.J. Martin, J. Massons, M. Aguilo and F. Diaz, **J. Luminescence** 79, 127-132, (1998).
24. N.V. Stus, S.N. Dub, D.A. Stratyckuk and V.V. Linsyak, **J. Alloys and Compounds** 366, L13-L15, (2004).
25. M. Roth, N. Angert, M. Tseitlin, G. Schwarzman and A. Zharov, **Optical Materials** 26 (4), 465-470, (2004).
26. M. Roth, N. Angert, M. Tseitlin and A. Alexadrovski, **Optical Materials** 16, 131-136, (2001).

27. W. Liu, H.Y. Shen, G.F. Zhang, D.Y. Zhang, G. Zhang, W.X. Lin, R.R. Zeng and C.H. Huang, **Optics Communications** 185, 191-196, (2000).
28. D.Y. Zhang, H.Y. Shen, W. Liu, W.Z. Chen, G.F. Zhang, G. Zhang, R.R. Zeng, C.H. Huang, W.X. Lin and J.K. Liang, , **J. Crystal Growth** 218, 98-102, (2000).
29. H. Hirai, T. Masui, N. Imanaka and G.Y. Adachi, **J. Alloys and Compounds** 374, 84-88, (2004).
30. L. Schwarz, M. Kloss, A. Rhoemann, U. Sasum and D. Haberlandl, **J. Alloys and Compounds** 275-277, 93-95, (1998).
31. M. Kloss, B. Finke, L. Schwarz and D. Haberlandl, **J. Luminescence** 72-74, 684-686, (1997).
32. L. Schwarz, B. Finke, M. Kloss, A. Rhormann, U. Sasum and D. Haberlandl, **J. Luminescence** 72-74, 257-259, (1997).
33. S. Lucas, E. Champion, D. Bregiroux, D. Bernache-Assolant and F. Audubert, **J. Solid State Chem.** 177, 1302-1311, (2004).
34. S. Lucas, E. Champion, D. Bernache-Assolant and G. Leroy, **J. Solid State Chem.** 177, 1312-1320, (2004).
35. H. Onada, H. Naraiai, H. Maki and I. Mtooka, **Materials Chemistry and Physics** 73, 19-23, (2002).
36. Z.S. Gonen, M. Kizilyalli and H.O. Pamuk, **J. Alloys and Compounds** 303-304, 416-420, (2000).
37. A. Uztetik- Amour and M. Kizilyalli, **J. Solid State Chem.** 120, 275-278, (1995).
38. U.D. Altermatt and I.D. Brown, **Acta Cryst.** A34, 125-130, (1987).
39. E. Husson, F. Genet, A. Lachar and Y. Piffard, **J. Solid State Chem.** 75, 305, (1988).
40. K. Nakamoto, **"Infrared Spectra of Inorganic Compounds"**, Wiley Interscience, NY 1971.